International Journal of Greenhouse Gas Control 99 (2020) 103085

Contents lists available at ScienceDirect

International Journal of Greenhouse Gas Control

journal homepage: www.elsevier.com/locate/ijggc

The correlation between pO_2 and pCO_2 as a chemical marker for detection of offshore CO_2 leakage

Christian Totland[a,*], Espen Eek[a], Ann E.A. Blomberg[a], Ivar-Kristian Waarum[a], Peer Fietzek[b], Axel Walta[a]

[a] Norwegian Geotechnical Institute, Sognsveien 72, 0806 Oslo, Norway
[b] Kongsberg Maritime GmbH, Hellgrundweg 109, 22525 Hamburg, Germany

ARTICLE INFO

Keywords:
Carbon capture and storage
Geological carbon storage
CO_2 leakage
Chemical detection
pH
AUV

ABSTRACT

A controlled CO_2 release experiment was carried out in order to mimic unintended leakage of geologically stored CO_2, and to study methods for detecting these leak events. The experiment was carried out at 60 m depth in the Oslo Fjord over the course of one month. During the simulated leak events, the water chemistry was monitored by sensors mounted on stationary templates located 10 and 22 m horizontally from the source, as well as sensors mounted on an Autonomous Underwater Vehicle (AUV). During baseline conditions (no CO_2 release), we observe a strong biogenic correlation between O_2 and CO_2. This correlation is lacking during CO_2 releases, indicating that the CO_2-O_2 correlation can be used as a marker for CO_2 leakage. The same deviations were not initially detected by the CO_2 sensor mounted on the AUV due to the longer response time of membrane-based CO_2 sensors. However, by applying response time correction in the post-processing of the AUV CO_2 data, the generated CO_2 plume was detected. Moreover, the plume was clearly detected by the AUV using the faster responding pH sensors, where the correlation with O_2 again could be used to confirm the anomaly.

1. Introduction

Permanent storage of carbon dioxide (CO_2) in geological formations has been proposed as a method to abate climate change. Suitable geological formations can isolate vast amounts of CO_2 from the atmosphere (Consoli and Wildgust, 2017), and several large-scale storage projects (several Mt/year) are in the planning stage worldwide (Institute, 2015; Jenkins et al., 2015). Moreover, a few dozen small-scale projects have already been successfully executed, storing from a few hundred to 1 million tons of CO_2 per year (CO2CRC, 2013; Jenkins et al., 2015). An important part of a CO_2 storage project is to verify that the injected CO_2 stays in the geological storage reservoir as intended. Since there is limited experience with long-term geological CO_2 storage, the need for monitoring to ensure storage integrity, is significant.

Seismic techniques can be used to verify that the injected CO_2 plume is well contained within the planned storage reservoir (Arts et al., 2004; Jenkins et al., 2015; Schacht and Jenkins, 2014). Seismic methods are well suited for long-term monitoring of the location and spatial extent of the injected CO_2 plume, and can give an early warning regarding large-scale leaks. Routine marine environmental monitoring of the water column is also recommended to verify that there are no indications of CO_2 reaching the seabed or the water column above the geological storage reservoir, and to promptly detect any leakage if it should occur (Atamanchuk et al., 2015; Blackford et al., 2014; Maeda et al., 2015; Myers et al., 2019; Shitashima et al., 2015; Uchimoto et al., 2018).

The water column above an offshore carbon storage site is part of an interconnected system including adjacent water masses, the seabed and the atmosphere; all affected by a vast number of physical, chemical and biological processes, not related to leakage of CO_2. Monitoring of any parameter in the water column therefore poses the considerable challenge of separating natural variability from variation caused by the storage activity (Blackford et al., 2017). For example, there will be considerable variation in water column CO_2 concertation due to organic matter (OM) degradation that has taken place in a specific parcel of water between the last time this parcel was equilibrated with the atmosphere and the time of determining the CO_2 concentration. The oxygen consumption caused by the degradation of OM will lead to a decrease in level of dissolved oxygen (DO) accompanying the CO_2 increase. This fundamental inverse correlation between O_2 and CO_2 will persist in the absence of any other source of CO_2 (Bickle, 2009; Ohtaki et al., 1993; Uchimoto et al., 2017, 2018), and can therefore be used to

* Corresponding author.
E-mail address: Christian.totland@ngi.no (C. Totland).

https://doi.org/10.1016/j.ijggc.2020.103085
Received 5 March 2020; Received in revised form 29 May 2020; Accepted 2 June 2020

discriminate the natural biotic variation in pCO_2 from variations caused by abiotic mechanisms. In addition to leakage from a geological carbon storage (GCS) site, abiotic mechanisms include for instance leakage of CO_2 from natural geological sources and dissolution of $CaCO_3$ in deep waters. Small variations in initial DO and pCO_2 in any water mass will also occur due to differences in temperature and salinity at the point where the water was equilibrated with the atmosphere. Variations in the correlation between these parameters can also be caused by small variations in the amount of oxygen utilized for each mole of carbon combusted by organisms. These variations would originate from variations in the properties of organic matter being combusted, such as the degree of oxidized functional groups in the available organic matter. These differences would be most important between water masses with very different origin and history before arriving at the point of monitoring.

Hence, in order to identify increased pCO_2 caused by a leakage, and to reduce the rate of false alarms, monitoring the co-variability of multiple chemical parameters is a good strategy. This has been suggested previously (Uchimoto et al., 2017, 2018); however, there is no consensus on which parameters should be monitored, or how anomalous variations can be positively separated from natural variability. Continued research efforts towards finding potential chemical signatures related to CO_2 leakage is therefore important, both to be able to verify the integrity of the storage formation and for public assurance.

Uchimoto et al. (2017&2018) argued that a constant pCO_2 threshold value will result in too many false positives or negatives, and suggested that the threshold should be adjusted with respect to the DO% in the specific marine environment. The basic idea is that waters with lower DO% require a higher pCO_2 threshold value compared to water with high DO%, hence a covariance threshold was proposed. The concept of using the pCO_2/pO_2 correlation to identify leaks was proposed in the QICS research project (Atamanchuk et al., 2015), where a reduction in the pCO_2/pO_2 correlation was observed when an external source of CO_2 was introduced. However, there is limited data on the pCO_2 and DO correlation during offshore simulated leakage experiments. Most studies on leakage detection in the water column have primarily focused on the elevated CO_2 levels and/or reduced pH levels associated with CO_2 leakage (Atamanchuk et al., 2015; Blackford et al., 2014; Maeda et al., 2015; Shitashima et al., 2015). Moreover, the possible advantages and disadvantages of mounting chemical sensors on autonomous vehicles versus on stationary platforms, resulting e.g. from differences in response characteristics of different sensors, needs further investigation. The fundamental oceanographic conditions with surface waters saturated with DO and CO_2 from the atmosphere (or supersaturation with DO from photosynthesis) and increasing pCO_2 and decreasing DO with depth normally causes variability with depth which is much stronger than the variability with time or position at a constant depth. This has consequences for the expected variability when monitoring with sensors on a stationary platform at a fixed depth in contrast to monitoring with a mobile unit.

Atamanchuk et al. (2015) and Maeda et al. (2015) reported on a controlled sub-seabed CO_2 release experiment conducted in the Ardmucknish Bay in Scotland. From this experiment, a negative correlation between DO and pCO_2 was found in the period without CO_2-release, where this coupling was found to be weaker during the periods with active release of CO_2 (Atamanchuk et al., 2015). This experiment was done at 12 m water depth and based on pCO_2 and DO measurements from a stationary platform with sensors 30 cm above the seabed located in the epicenter of the CO_2-release. The experiment therefore does not explore the ability to detect leakage by monitoring the pCO_2-O_2 correlation from stationary platforms located at a distance from the leakage point. It would further be useful to verify whether the decoupling of the negative pCO_2-DO correlation can be used to identify abiotic CO_2-release in a more exposed offshore area. Maeda et al. (2015) reported results from the same bay using an autonomous underwater vehicle (AUV), where detection of the low-pH plume was found to be sensitive to the large tidal variations in the bay, with low detectability during flood tide. Simulations suggested that a decrease in pH caused by released CO_2 will be restricted to the immediate vicinity of the leakage (Maeda et al., 2015).

In order to evaluate the ability of sensor combinations mounted on different platforms to detect anomalous environmental variation in the water column linked to CO_2 leakage, artificial CO_2 leakage events were created over the course of one month in an exposed nearshore environment in the Oslo fjord, at 60 m depth. The CO_2 release consisted of both gas bubbles and release of CO_2 enriched seawater simulating evacuation of pore water. The latter leakage scenario can occur when CO_2 migrates upwards in the formations and dissolves and pushes pore water towards the seabed (Kampman et al., 2014). Due to the potentially different chemistry of pore water, such as e.g. varying salinity, this can result in different chemical signatures than the release of CO_2 gas only. In this study, the salinity of the released artificial pore water is varied, which will influence its density, and thereby its movement and location in the water column.

The response to the controlled release of CO_2 was measured using chemical and acoustic sensors mounted on sensor templates on the seabed, and on an Autonomous Underwater Vehicle (AUV). This paper covers the results related to the chemical sensors. The monitored parameters include pCO_2, pO_2, salinity and pH. Particular focus is put on the covariance of pCO_2 and pO_2 as a chemical signature for leakage detection. Additionally, currents in the water column were continuously monitored to interpret the movement of potential plumes and water masses that have different CO_2-O_2 signatures.

2. Experimental section

2.1. Test site and experimental setup

The CO_2 leakage experiment was done outside the Østøya Island outside Horten in the outer part of the Oslo fjord (Fig. 2), from the 7th to 30th of May, 2019. The water column at this site is characterized by a salinity gradient due to fresh water entering the fjord from several rivers (Fig. 1). Hence, the surface water is characterized by brackish low-salinity water (salinity about 15), with a steep salinity gradient for the first 10 m of the water column (Fig. 1). The test site was located at 60 m depth, and for the bottom 20 m the salinity is approximately constant around 35.

Fig. 2 illustrates the experimental setup. CO_2 was released as gas and as CO_2 enriched seawater at 60 m water depth, 100 m from the shore. CO_2 in gas- and dissolved phase was released about 1 m above

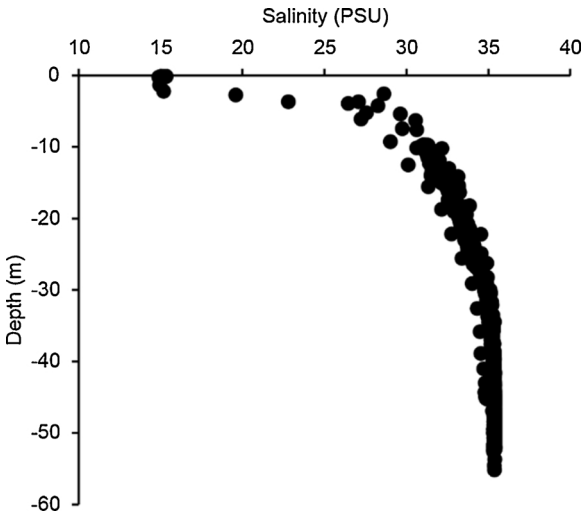

Fig. 1. Salinity in the water column at the test site recorded with the HUGIN AUV on May 21st 2019.

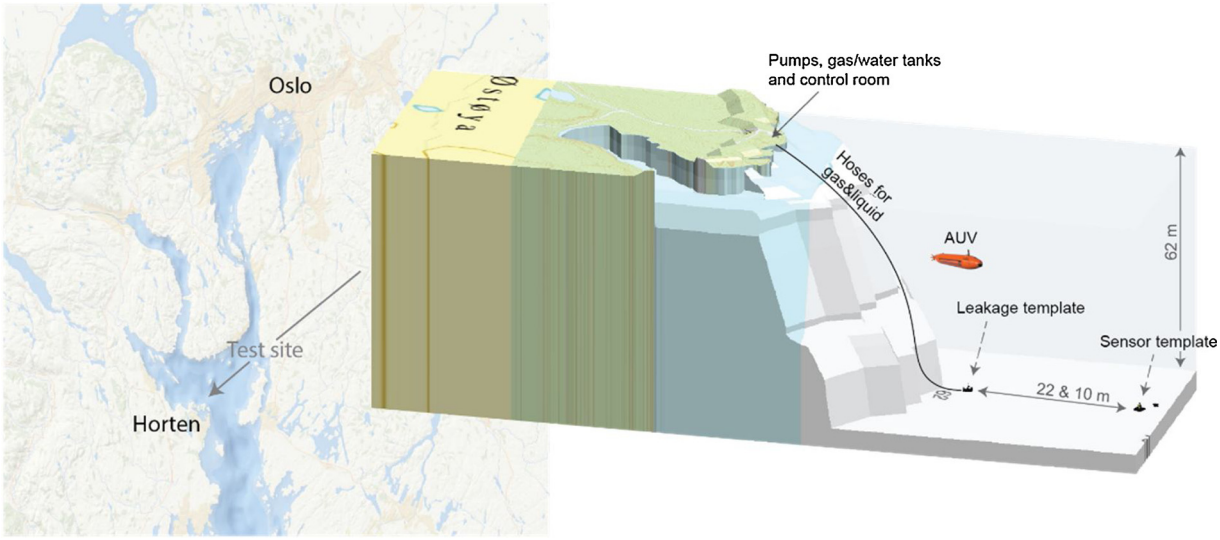

Fig. 2. Test site location and schematic presentation of the experimental setup. The figure displays a 22 m distance between the leakage and sensor templates; however, this distance was reduced to 10 m for one day of leakage experiments. The scales (except the AUV) are realistic.

the seabed through pipes mounted on a seabed template connected to onshore feed tanks. Gas phase CO_2 was released from pressurized gas tanks fitted with a pressure regulator and a flowmeter. The CO_2 enriched seawater was prepared in 1 m^3 mixing tanks. Seawater from 6 m depth (Salinity = 23.5, T = 9 °C) was pumped into the tanks and purged with CO_2-gas. Natural sea salt (GC Rieber) was added while the water in the tank was continuously mixed with a submersible pump, in order to adjust the salinity to the desired level.

The CO_2-enriched water was pumped from the tank to the release point at the leakage template while continuously monitoring the flow. Before releasing the water, pH, salinity and temperature was recorded for each batch. The pCO_2 of the released water was calculated using the Aqion hydrochemistry software. Three onshore tanks of 1000 L each were used, where the water was released consecutively to achieve a total of 3000 L per release experiment.

The created CO_2 leakage scenarios varied in size (see the results section), but corresponded to small leakages of less than 1 T/d.

The gas was released from a 3 mm diameter opening. The size of the bubbles were determined both by a laboratory set-up at 6 m depth, where a video of the gas release was analysed using Matlab image processing software, as well as by visual inspection during the actual near shore tests at 60 m depth. The average bubble diameter determined in the laboratory was about 1 mm, with a size distribution ranging from about 0.5–6 mm, and the visual inspection during the near shore tests executed for this study indicated a similar average bubble size.

2.2. Sensors

Chemical sensors (pCO_2, pH, pO_2, salinity (S) and temperature (T)) mounted on a seabed template recorded data throughout the test period. The sensors ran continuously with sample rates of every second (pH, S, T), every 30 s (pCO_2) and every minute (pO_2). The sensor template was at the beginning of the experiment placed 22 m northeast of the leak point. On May 21st the sensor frame was moved and placed 10 m northeast of the leakage frame. The HUGIN AUV with pH, pCO_2, pO_2, S and T sensors was used for one day to measure chemical parameters above the CO_2-leakage point.

The CONTROS HydroC CO_2 is a submersible (down to 6000 m) pCO_2 sensor that combines membrane equilibration of an internal headspace with optical, NDIR-based gas detection. The sensor design and the applied calibration are originally described in Fietzek et al., 2014. The power consumption is around 4 W (excluding the underwater pump) and response time with pump and flow-head is approximately 60 s (τ_{63}). The manufacturer states the initial accuracy of the sensor to be ± 0.5 % of reading and Fietzek et al., 2014 assessed an accuracy of < 4 µatm for multi-week, processed, in situ sensor data. Regular, internal zero-gas measurements enable an in situ response time determination and signal drift correction (Fietzek et al., 2014).

The CONTROS HydroFlash O_2 was an optical, fluorescence quenching based pO_2 sensor, i.e. an optode, with a depth rating of 6000 m. An optode technology review is given by (Bittig et al., 2018). This sensor had a power consumption of 0.1 J per sample and a fast response time of (τ_{63} < 3 s). The optodes were by default calibrated in a water tank following a multi-point temperature and O_2 calibration matrix for a measuring range of 0–300 mbar. The manufacturer stated an accuracy of ± 1 mbar or 1.5 % of reading (whichever is greater) and recommended a re-calibration after 12 months.

The pH sensor has a reported response time of 3 s (τ_{63}), drift of 0.05 pH/month, accuracy of 0.01 and resolution of 0.001 pH units. The sensor is operational up to 700 bar.

3. Results and discussion

The artificial leakage scenarios were monitored by both stationary and mobile sensors. The results are presented and discussed in separate subsections below. Some data are presented in more detail in the Supplementary Materials. This includes the baseline data and AUV travel path.

3.1. Response from stationary sensors

3.1.1. pCO_2 and pO_2 covariance

Fig. 4 ii) shows that the natural variation in pCO_2 is 40 µatm for the entire period of testing. During a single day, the baseline variation for pCO_2 was around 30 µatm (Figs. 3A and 4 i)). In comparison, the variation in pCO_2 during the artificial CO_2 leakage events ranged between 5 and 35 µatm. Consequently, identifying anomalous variation in pCO_2 would not be possible by only looking for increases in pCO_2. The baseline correlation between pCO_2 and pO_2 is very good (Figs. 3A and 4), reflecting that the principal mechanisms for variation in pCO_2 and pO_2 are biogenic processes. Despite introduction of new water bodies at the sensor site with varying salinity, temperature or O_2, pCO_2 and pO_2 remain well correlated. This shows that the baseline correlation is very stable over the different water masses mixing in this area. This means that although these water masses could have slightly different history

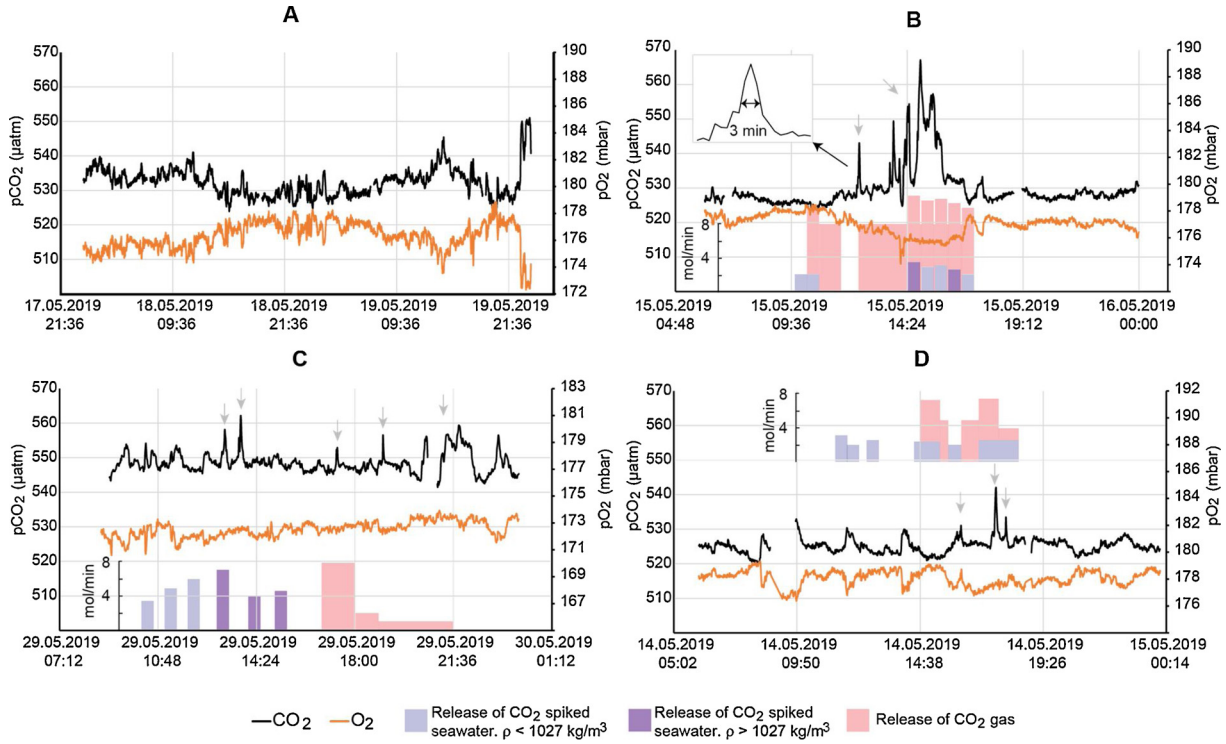

Fig. 3. The covariance of pCO_2 and pO_2 measured at the sensor template. The sensor template was located 22 m from the leak point until May 21st 2019, after which it was moved to a 10 m distance; i.e. plot **B** and **D** illustrate the response from sensors located at a 22 m distance from the leak, whereas plot **C** illustrates the response when sensors are located 10 m from the leak point. Plot **A** illustrates the baseline conditions with biogenic covariance of pCO_2 and pO_2. No significant deviation from this covariance was observed during the one month of measurements, except during the artificial CO_2 release experiments (plots **B**-**D**). The rate of CO_2 released during the experiments is indicated in the plots (mole CO_2/min), as well as the type of medium used, i.e. CO_2 gas and/or CO_2-spiked high-salinity or low-salinity seawater. Note that the upper limit of the flow meter used to monitor the gas release correspond to 8 mol/min, and the flow rate exceeded this limit in plot B and C. Hence, the exact amount of gas released these days is unknown, except that it exceeded 8 mol/min. The low-salinity seawater had a salinity around 23.5, whereas the high-salinity water had a salinity between 35 and 44. The baseline salinity around the sensors were around 34.

with respect to amount and composition of organic matter and content of DIC and DO at equilibrium with the atmosphere, the effect of these differences is small on the relationship between pO_2 and pCO_2.

However, during leakage events, deviation from this correlation is observed. During the release experiments, several different leakage scenarios were simulated, where the CO_2 was either pre-dissolved in seawater prior to release (to simulate CO_2 saturated pore water), released as gas, or released as both gas and dissolved in seawater simultaneously. For the experiments shown in Fig. 3 C, CO_2 gas and CO_2 dissolved in seawater was released systematically. Our observations indicate that both CO_2 gas and dissolved CO_2 creates anomalous CO_2 spikes in the water near the sensor template (indicated with arrows in the figure for clarity).

Other induced variables include the salinity of the released seawater and the quantity of released CO_2. Additionally, release experiments were conducted with the sensor template located 10 or 22 m from the leak point in order to study any effects of distance. The variables that can affect the measured responses are discussed individually below.

3.1.2. *Mobility of the generated CO_2 plume: Currents and diffusivity*

At the test site, there was no distinct current direction in the bottom part of the water column (Fig. 5), for most days of experiments. However, for one of the experiment days (May 29th), there was primarily an eastbound current direction. The average current strength and direction for the entire period of measurements (May 7th to May 29th) show that the water masses overall move eastwards, but with substantial movement in all directions. The sensor template is located northeast of the leak point (Fig. 5). It is known that the estuarine circulation in the Oslo

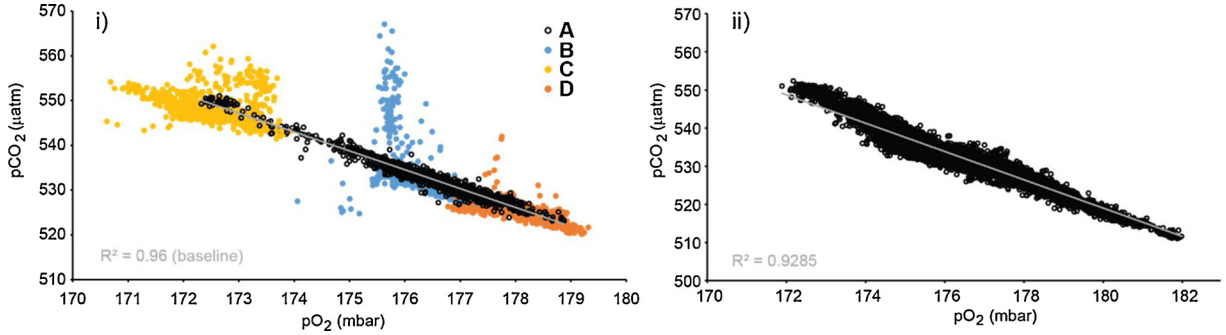

Fig. 4. i) Scatter plots illustrating the correlation between CO_2 and O_2 for the periods displayed in Fig. 3 **A** – **D**. **A** represents baseline conditions for a single day, whereas **B**, **C** and **D** represent days (12 h from the onset of a leakage event) where various artificial CO_2 leakage events occurred. See Fig. 3 for more details regarding the leakage scenarios. **ii)** The right plot shows the correlation for the baseline, i.e. during sixteen days where no leakage experiments were performed.

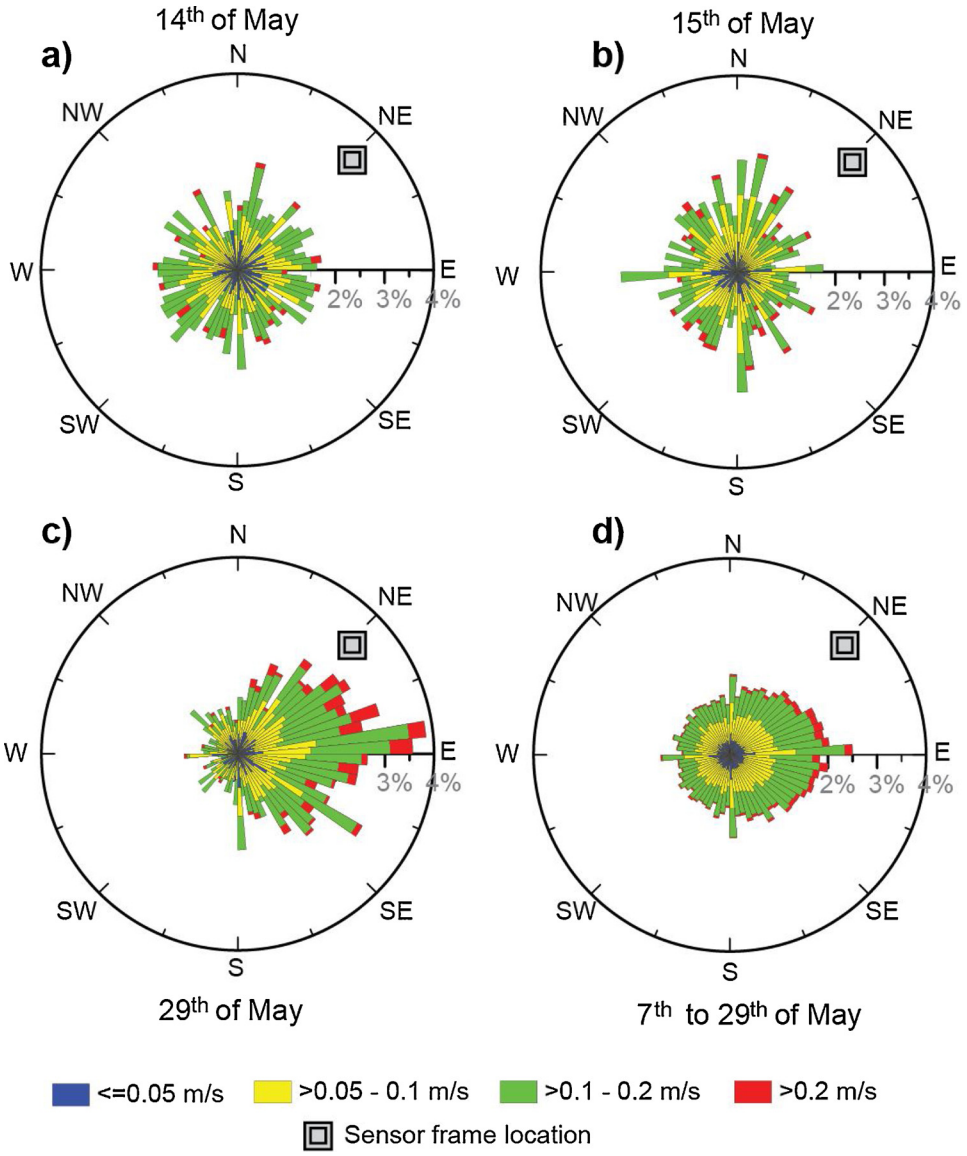

Fig. 5. Rose charts describing the current conditions 1.5 m above the leakage frame during three days of leakage experiments (**a**), **b)** and **c)**), as well as during the entire period of measurements **(d)**. The Aquadopp current profiler was placed on the sensor template. The location of the sensor template northeast of the leak template (imagined in the center of the charts) is indicated in the charts for clarity.

fjord predominantly is limited to the upper 20 m, and that replenishment of the deeper waters mainly occurs during winter (this study was conducted during spring) (Gade, 1968). The general absence of a persistent current direction in the bottom waters was also visually observed via a camera mounted on the gas/liquid leak template, where particles moved back and forth in the water masses, rather than in a specific direction. Hence, at this location, it can be more relevant to estimate the mixing of the released CO_2 into the surrounding water masses and transport of the plume influenced by the CO_2-release assuming an eddy diffusion mechanism and back and forth movement of water masses, and not unidirectional currents.

It is difficult to evaluate the time between CO_2 release and response. Conditions may vary slightly between experiments, and on the small scale of 10–22 m between the leak point and the sensor template, multidirectional flow (water moving back and forth) can be important in determining the timing, concentration and volume of the plume that reaches the sensors. This is believed to be the reason it is difficult to see any regularity in the time between CO_2 release and sensor response (see e.g. Table 1). Moreover, the evacuation of gas and liquid at the leak point will generate additional turbulence and affect the transport of the plume. The time between initiation of leakage and first observed response was 1.5 and 5.5 h with a 22 m distance between leak point and sensors, and 3.5 h when the distance was 10 m. However, it is reasonable to assume that not all generated plumes will travel past the sensors, due to e.g. differences in plume density (see next section), and it is

Table 1
Specifications of the sensors used in the experiments.

Sensor platform	Sensors
Stationary sensor template	CONTROS HydroC[a], CO_2
	CONTROS HydroFlash[b], O_2
	Ocean Seven multisensor[c] (pH, S and T)
Stationary leakage template	Aquadopp current profiler[d]
HUGIN AUV	CONTROS HydroC[a], CO_2
	CONTROS HydroFlash[b], O_2
	Ocean Seven, pH probe[c]

[a] 4H-JENA engineering GmbH, Jena, Germany.
[b] Formerly Kongsberg Maritime Contros GmbH, Kiel, Germany.
[c] IDRONAUT S.R.L., Brugherio, Italy.
[d] Nortek AS, Rud, Norway.

Table 2
Details regarding released CO_2 and responses for experiments conducted the 29th of May 2019 (Fig. 3C), as well as calculated densities of the released CO_2-spiked artificial pore waters, and integrals of the responses (Millero et al., 1980; Ohsumi et al., 1992). The background density at the site was 1027 kg/m^3. Each release consisted of about 1 000 L of water.

Times of release	CO_2 state	Mol CO_2 /min	Salinity (psu)	Density (kg/m^3)	Time intervals of sensor response	Integral of response (pCO_2, µatm s^{-1})
10:14–10:38	Dissolved	2.7	19	1016.3	13:15–13:22	9300
11:09–11:36		4.6	23	1020.2	13:44–13:54	8850
12:38–13:05		5.8	27	1023.6	17:16–17:24	4400
13:09–13:37		6.1	33	1028.5	18:59–19:05	3350
14:10–14:37		3.4	38	1031.4	20:25–20:39	7750
15:07–15:34		3.9	44	1036.4	21:00–22:23	46,400
16:07 - ca. 17:00	Gas	> 8*	–	–	23:06–23:19	7150
ca. 17:00 - ca. 21:00		1 – 2	–	–		

* The flow of CO_2 exceeded the measurement limit of the flow meter. Hence, the exact amount of CO_2 released during this time is not known, except it likely corresponded to significantly more than 8 mol/min.

therefore difficult to assess which of several consecutive releases on the same day that generated a response from these data.

The assumed travel time of the plumes indicates a horizontal diffusivity in the order of 10^{-4} m^2/s, in which the plume would take about 40 min to travel the 22 m. This is comparable to the vertical diffusivity of 2×10^{-4} m^2/s measured at these depths in the Oslo fjord previously (Røed, 2016).

It is interesting to note that the CO_2 response typically occurs as relatively narrow spikes in the time plots, where the elevated non-biogenic CO_2 level is detected only for a few minutes (Fig. 3B and Table 2). We interpret this as a spatially defined CO_2 plume passing the sensors, which is consistent with a combination of eddy diffusive mixing and small scale multi-directional flow. However, when large amounts of CO_2 gas were released over several hours, a more prolonged response was observed (Fig. 3B&C and Table 2).

In general, the total amount of released CO_2 corresponds reasonably well to the magnitude of the sensor response (Fig. 3 and Table 2). Table 2 gives the integrals of CO_2 spikes observed the 29th of May 2019 (Fig. 2C). This integral is roughly proportional to the amount of CO_2 passing through the water volume around the sensor. The largest integral of 46 400 µatm is connected to a larger and continuous release of CO_2 gas prior to the response. In this case, the quantity of released CO_2 is reflected in the size of the response, relative to the other responses measured this day. Further, the large quantity of CO_2 released the 15th of May 2019 (Fig. 3B) generated a similar response (I ~ 50 000 µatm). Fig. 5 shows that the dominant current direction was different these two days, with no dominating current direction on the 15th, and a primarily eastbound current direction on the 29th. The current conditions were similar the 14th and 15th of May, and these days are therefore more comparable, although more CO_2 was released on the 15th compared to the 14th of May. The exact amount of CO_2 released as gas is not known, as the flow rate exceeded the upper limit of the flow meter. However, the response is nearly six times larger on the 15th. The results indicate that variations in the conditions that control the eddy diffusivity and mobility of the plume, as well as properties of the plume itself, can have a significant impact on what sensors located a distance from the leakage will measure. This is probably especially true in the relatively calm waters where our release experiments were performed. Current legislation for GCS states that quantification of a leakage is mandatory, despite no existing consensus on how this quantification should be performed. This work shows that through the simultaneous measurement of pCO_2 and pO_2 it is possible to discriminate between increases in CO_2 concentration with natural biogenic origin and increases caused by introduction of abiotic CO_2. Furthermore, the indicated correspondence between response on a single sensor and the quantity of released CO_2 means that this is a potential way forward to find a method for leakage quantification from chemical water column monitoring.

3.1.3. *Effects of pore water salinity and density*

It was hypothesized that a denser plume will affect the sensors mounted on a seabed template to a greater extent than lighter plumes. The former can occur when CO_2 dissolves in high-salinity pore water on its path from the storage formation to the sea floor, or when sufficient amount of CO_2 dissolves in seawater above the seabed to increase the density of this water. The higher density of this water will cause the plume to accumulate at the bottom. The opposite scenario can occur if the leakage path passes through aquifers with fresh or brackish water. In the event of leakage, evacuation of CO_2 can occur both as gas and CO_2-spiked pore water, and displaced pore water can potentially leak for an extended period prior to the occurrence of bubbles (Chabora and Benson, 2009; Pruess, 2011). The salinity of the released CO_2-enriched water was in our experiments varied between 19 and 44, and the ambient salinity at sensor installation depth was around 34. For the six 1 000 L batches of CO_2-enriched water released the 29th of May 2019 (Fig. 3C), the salinity was increased gradually (19, 23, 27, 33, 38 and 44). The density of the released water was calculated based on measured temperature, pressure, salinity and pCO_2 (Table 2) (Millero et al., 1980; Ohsumi et al., 1992). Six and forty minutes following the release of CO_2 enriched water with a density of 1028.5 kg/m^3, narrow CO_2 peaks were observed that break the CO_2 – O_2 biogenic correlation (the ambient water density is 1027 kg/m^3). However, there was no apparent sensor response following release of higher density water (1031.4 and 1036.4 kg/m^3) on the 29th, as well as on the 15th of May (Fig. 3B and C). A possible explanation for this is that the denser plumes travel below the sensors, which are mounted at one meter height.

The plumes generated by release of CO_2 gas alone will also be slightly denser than the surrounding waters due to a density increase upon CO_2 dissolution (Ohsumi et al., 1992). However, this density effect caused by CO_2 gas dissolving and mixing with the surrounding water is small compared to the density differences due to salinity variation. As the CO_2 bubbles rise, the CO_2 is mixed into slightly less dense water further up in the water column. This means that the gas release of CO_2 can result in CO_2-rich water with both slightly higher and similar densities than the water at the depth of release. Further up in the water column, the CO_2-enriched water can be less dense as well. The data show that the release of CO_2 gas alone is detected by the stationary sensors (e.g. Fig. 3C) and this is consistent with a plume of CO_2-enriched water of similar or slightly elevated density compared to the water at the release depth.

3.1.4. *pH responses*

pH correlates inversely with pCO_2 as a consequence of the reaction of CO_2 with water. Hence, a correlation between pH and pO_2, as between pCO_2 and pO_2, can be expected. This correlation can therefore be an alternative chemical signature for detecting CO_2 leakage. The largest response in pCO_2 detected during the release experiments, was a change of about 35 µatm (Fig. 3B). Fig. 6 below shows that this

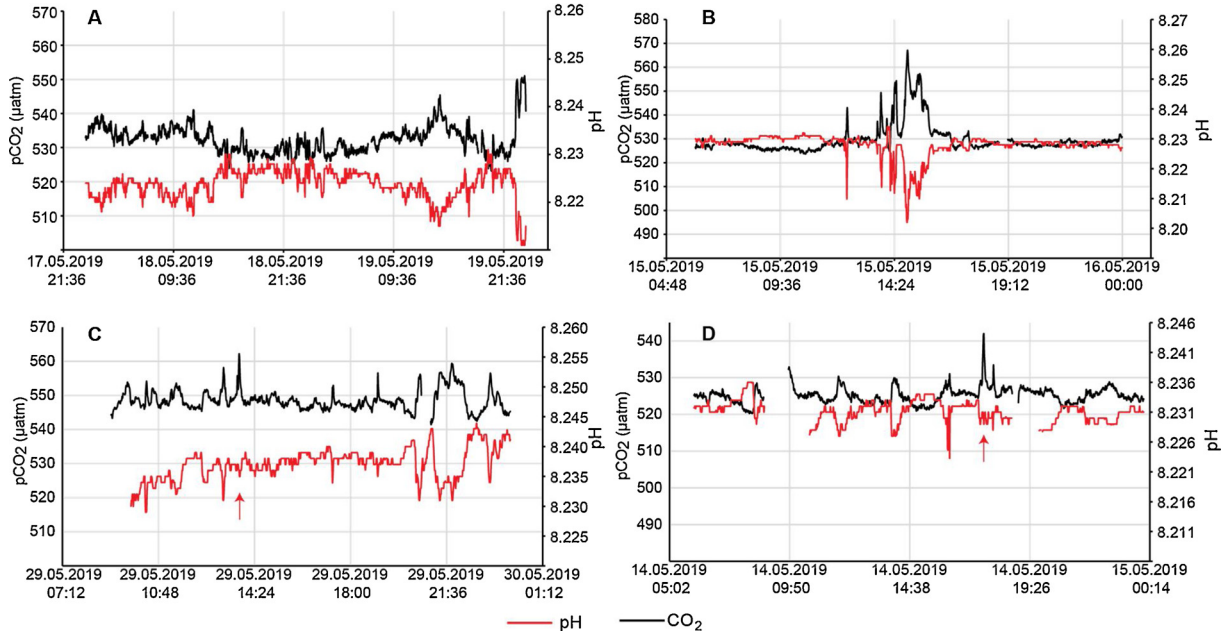

Fig. 6. The covariance of pH and pCO_2 measured by sensors mounted on a seabed template. The sensor template was located 22 m from the artificial CO_2 leakage until May 21st 2019, after which it was moved to a 10 m distance; i.e. plot **B** and **D** illustrate the response from sensors located at a 25 m distance from the leak, whereas plot **C** illustrates the response when sensors are located 8 m from the leak. Plot **A** illustrates the baseline conditions with biogenic covariance of pCO_2 and pH. CO_2 release experiments were conducted during the days corresponding to plots **B**-**D** (see Fig. 3 for details). The drops and cut-offs in pH seen in plot **D** are due to sensor shutdowns.

response corresponds to a change in pH of less than 0.03. This observation supports the observations and simulations done by Maeda et al. (2015), who showed that a low-pH plume will not diffuse to a wide area, and that only small changes in pH can be expected at a certain distance from the leak (Maeda et al., 2015). In our experiment, a change in pH of maximum 0.03 is achieved by releasing CO_2 corresponding a leakage between 0.5 and 1 T/d, at a 22 m distance from the sensors. This corresponds fairly well to the results of the modelling conducted by Blackford et al. (2020), where it was suggested that a 1 T/d release could lead to a decrease in pH of 0.01 up to a 60 m distance from the leakage point. During a larger leakage event, a more concentrated plume may occur over a wider area, which in turn will affect pH further (Blackford et al., 2020; Caramanna et al., 2011; Phelps et al., 2015).

Fig. 6 C and D further show two anomalous CO_2 spikes that do not give a clear corresponding response in pH. These are marked with red arrows in Fig. 6. A possible explanation for this is that the HydroC CO_2 sensor uses a pump, and thereby senses a larger water volume, which averages the measurement to some extent. Moreover, the different placements of the sensors on the stationary template may be sufficient to put the pH sensor just outside the plume. However, the explanation for this observation is not clear.

A key characteristic of electrochemical pH sensors is their quick response time compared to membrane-based CO_2 sensors. On the other hand, they have a notable drift, which may be an issue for long-term deployment. The response time of the pCO_2 sensor used for this study was estimated at around two minutes (τ90), whereas the response in the electrochemical pH sensors is only a few seconds. Hence, the CO_2 sensor needs to be exposed to the plume for a longer period in order to report a correct value. This is generally not an issue for sensors mounted on stationary templates; however, for mobile units like AUVs and gliders, where the sensor potentially can pass through the plume in a matter of seconds, the quick response time of the pH sensors can be an advantage. An option to enhance the detection capability when using membrane-based CO_2 sensors on mobile units, is to apply response time correction (RTC) during post processing (Atamanchuk et al., 2015; Fiedler et al., 2013; Fietzek et al., 2014). This option is explored in the next section, where data recorded by sensors mounted on an AUV are discussed.

3.2. AUV sensor responses

Proposed monitoring strategies for the detection of anomalies related to CO_2 leakage often include AUVs to perform spatially resolved surveys and to cover larger areas (Blackford et al., 2015). Here, the HUGIN AUV from Kongsberg Maritime was equipped with multiple sensors including CTD, pH, O_2 and CO_2 sensors, and performed measurements at various depths and distances from the leakage point, at a speed of 1.5 m/sec. Fig. 7 shows measurements acquired during a leakage event, where the AUV passed by the leak point several times, at approximately 10 m vertical distance. From the 3D plot shown in Fig. 7 A, a narrow area with reduced pH is clearly visible over the point of the leakage (indicated with a circle). Fig. 8 A show the same data in a 2D time plot, where the regular negative spikes in pH are clearly visible, which occur when the AUV passes through the CO_2 plume. Moreover, the anomaly of the pH variation is further supported by the break in the pH - O_2 correlation (Fig. 8A). Hence, the presence of a plume is clearly indicated by the pH measurements. Still, no variation indicative of leakage is seen from the raw data of the pCO_2 sensor (Fig. 7 B). The observed variation in pCO_2 is dominated by the natural vertical variation in pCO_2 and the depth variations done by the AUV during turns.

According to the pH data, the AUV passes through the plume in a matter of 10–15 seconds. Because the response time of the CO_2 sensor is two minutes (τ90, tested in the laboratory), the sensor will not reach the equilibrated value in this time frame. Consequently, the sensor does not generate a signal elevated from the ambient pCO_2 noise, and the plume is not detected.

The time lag of the CO_2 sensor can to a certain extent be compensated for through post-processing using a numerical inversion algorithm (Atamanchuk et al., 2015; Miloshevich et al., 2004). This response time correction (RTC) was applied to the raw pCO_2 data, and the results are shown in Fig. 7C and 8B. It is clear that spikes in pCO_2 align reasonably well with the negative spikes in pH, and that the plume is detected after the RTC post-processing is applied. However, it should be noted that the

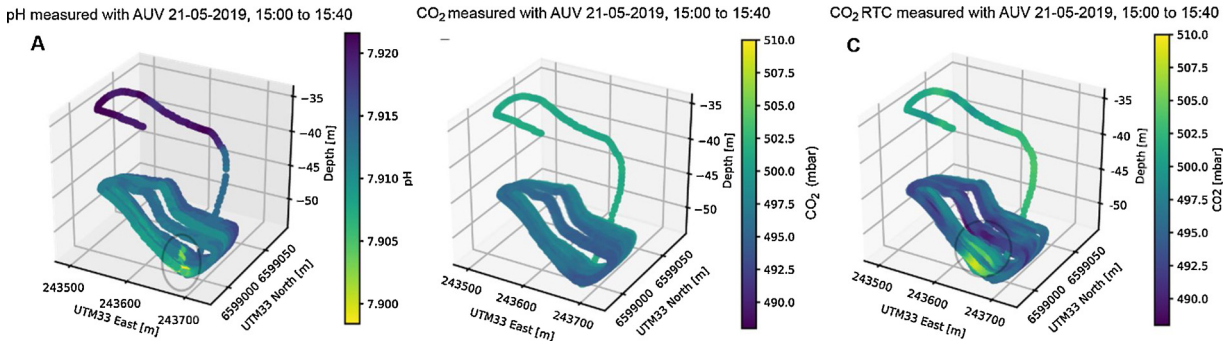

Fig. 7. Travel path and measurements of pH (**A**), pCO_2 (**B**) and pCO_2 following RTC post-processing (**C**), done with the AUV HUGIN during CO_2 leakage events. **B** show the pCO_2 raw data, i.e. no RTC is performed. The AUV travelled along a pre-programmed path, making nine passes of the leak template at a near constant depth of 50 m (i.e. 10 m above the leakage template); however, during 180 degree turns, the AUV will temporarily rise about 5 m higher in the water column. The AUV was moving at 1.5 m/sec. During the depicted time period, release of both CO_2-spiked seawater with ambient (relative to the release point) salinity and density, as well as CO_2 gas occurred continuously.

RTC-corrected CO_2 data appears noisier after this processing step. This is an artefact of the processing and may hamper data interpretation to some extent.

With a speed of 1.5 m/s, the pH response duration of 10–15 seconds indicates that the plume is around 20 m in diameter 10 m above the leakage nozzle. This implies that the plume is quite diluted and in part explains the relatively low drop in pH of around 0.01 to 0.02. This is similar to the observations from the stationary templates on other days of leakage experiments. A comparatively lower pH response is expected due to the buffer capacity of seawater.

The CO_2 releases conducted for this study correspond to a small leakage of about 0.5 T/d (assuming a continuous release). It was recently suggested that the plume rise height during smaller leaks (> 1 T/d) will predominantly be limited to 2 − 3 m above the seabed, and that AUVs therefore may not detect such leakage due to constraints on safe operational height for AUVs of 5 m above seabed (Blackford et al., 2020). However, as shown here, where the AUV travelled about 10 m above the leakage point, AUVs can be able to detect small leakages. Blackford et al. (2020) suggested that release events in shallow, well mixed systems may affect water higher above the sea bed.

On this particular day, no anomalies were detected using sensors on the stationary template. Note that loss of power supply prevented data collection from the stationary templates for parts of the day of the AUV measurements.

In summary, our results suggest the vehicle should move as close to the seabed as possible to detect chemical anomalies, and at low speed. The sensor sampling rate should be as high as possible to avoid moving through a CO_2 plume without registering it. In order to cover large areas during screening surveys to locate possible risk zones, mobile units are essential. However, for continuous or periodic monitoring of a spatially limited focus area such as an injection well, a stationary seabed template equipped with sensors can reliably detect signs of leakage or verify the opposite.

4. Conclusions

Geological carbon storage is generally considered a safe method for significantly reducing the amount of CO_2 released into the atmosphere, with a low risk of negative impact on the marine environment. Still, efficient methods for monitoring geologically stored CO_2 is imperative for the development of large-scale storage projects, both for storage integrity monitoring and for public assurance that the CO_2 stays in the reservoir as intended.

We found that the correlation between O_2 and CO_2 is a much better marker than increased CO_2 levels alone, in order to detect a potential CO_2 leak. In the study presented here, the measured increase in CO_2 related to the controlled release was within the natural variability range (at a constant depth), but still detectable because of the lack of CO_2-O_2 correlation. It is to be expected that seasonal variations in pCO_2 will be larger still. By using the CO_2-O_2 correlation as a chemical marker for

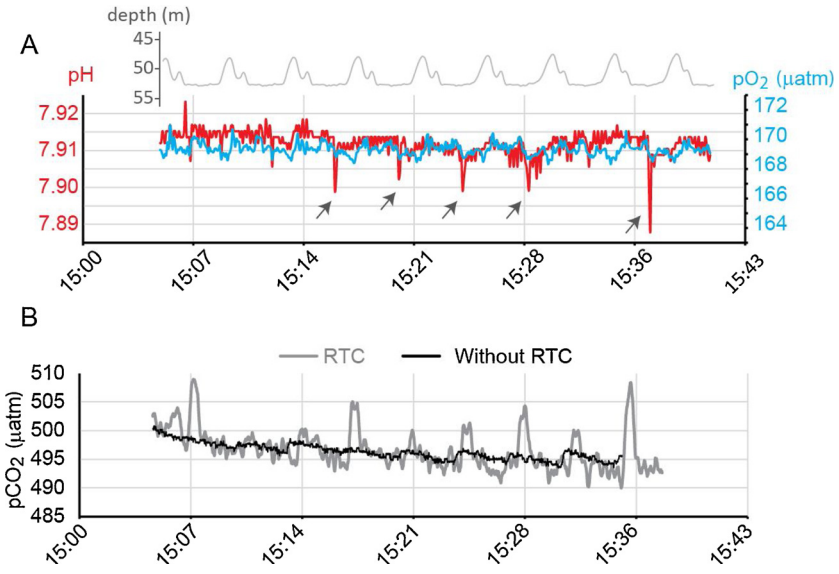

Fig. 8. A: Time plots of pH and O_2 which highlight the anomalous drops in pH when the AUV passed through the plume (see Fig. 7A). The pH anomaly is indicated with arrows. **B** shows the raw pCO_2 response (black line), as well as the response after response time correction (RTC) is applied to the raw data (gray line). During the depicted time period, release of both CO_2-spiked seawater with ambient (relative to the release point) salinity and density, as well as CO_2 gas occurred continuously.

CO_2 leakage, it is not necessary to know or estimate the geochemical conditions over a large area beforehand, since the method does not rely background CO_2, O_2 or pH levels.

In order to use this relationship to safely identify anomalies that deserve attention and further investigation, it is necessary also to assess the expected range of the natural relationship between pCO_2 and pO_2, or between pH and pO_2. Fig. 4 ii) shows the plot of pCO_2 vs pO_2 for the entire period of measurements, but without data from days where leakage experiments were done. This plot demonstrates the strong correlation between pO_2 and pCO_2 at this site, as well as the significant natural variability in these parameters in a single point of measurement.

Mobile sensor platforms, such as AUVs or gliders, can monitor a wide area, and are therefore attractive platforms for leakage monitoring. However, this study shows that the natural lateral and vertical variation in chemical parameters poses a challenge to interpretation of sensor data, and to the sensor specifications. Despite the natural vertical variation experienced by the mobile units, a deviation in the CO_2/O_2 correlation will still indicate leakage. However, monitoring of the equivalent pH/O_2 correlation, in addition to the CO_2/O_2 correlation, is recommended for the mobile platforms due to the slower response of the membrane-based CO_2 sensors.

Funding sources

This study was carried out as part of the ACT4storage project, funded through the CLIMIT program managed by Gassnova.

CRediT authorship contribution statement

Christian Totland: Writing - original draft, Investigation, Conceptualization. **Espen Eek:** Investigation, Conceptualization. **Ann E.A. Blomberg:** Investigation, Conceptualization, Project administration. **Ivar-Kristian Waarum:** Investigation, Formal analysis, Software. **Peer Fietzek:** Formal analysis. **Axel Walta:** Investigation.

Declaration of Competing Interest

The authors declare that they have no known competing financial interests or personal relationships that could have appeared to influence the work reported in this paper.

Acknowledgements

The authors kindly thank the HUGIN AUV operators and FFI for their contributions, and Kongsberg Maritime for helpful input regarding their chemical sensors.

Appendix A. Supplementary data

Supplementary material related to this article can be found, in the online version, at doi:https://doi.org/10.1016/j.ijggc.2020.103085.

References

Arts, R., Eiken, O., Chadwick, A., Zweigel, P., van der Meer, L., Zinszner, B., 2004. Monitoring of CO2 injected at Sleipner using time-lapse seismic data. Energy 29, 1383–1392.

Atamanchuk, D., Tengberg, A., Aleynik, D., Fietzek, P., Shitashima, K., Lichtschlag, A., Hall, P.O.J., Stahl, H., 2015. Detection of CO2 leakage from a simulated sub-seabed storage site using three different types of pCO2 sensors. Int. J. Greenh. Gas Control. 38, 121–134.

Bickle, M.J., 2009. Geological carbon storage. Nat. Geosci. 2, 815.

Bittig, H.C., Körtzinger, A., Neill, C., van Ooijen, E., Plant, J.N., Hahn, J., Johnson, K.S., Yang, B., Emerson, S.R., 2018. Oxygen optode sensors: principle, characterization, calibration, and application in the ocean. Front. Mar. Sci. 4.

Blackford, J., Stahl, H., Bull, J.M., Bergès, B.J.P., Cevatoglu, M., Lichtschlag, A., Connelly, D., James, R.H., Kita, J., Long, D., Naylor, M., Shitashima, K., Smith, D., Taylor, P., Wright, I., Akhurst, M., Chen, B., Gernon, T.M., Hauton, C., Hayashi, M., Kaieda, H., Leighton, T.G., Sato, T., Sayer, M.D.J., Suzumura, M., Tait, K., Vardy, M.E., White, P.R., Widdicombe, S., 2014. Detection and impacts of leakage from sub-seafloor deep geological carbon dioxide storage. Nat. Clim. Change 4, 1011–1016.

Blackford, J., Bull, J.M., Cevatoglu, M., Connelly, D., Hauton, C., James, R.H., Lichtschlag, A., Stahl, H., Widdicombe, S., Wright, I.C., 2015. Marine baseline and monitoring strategies for carbon dioxide capture and storage (CCS). Int. J. Greenh. Gas Control. 38, 221–229.

Blackford, J., Artioli, Y., Clark, J., de Mora, L., 2017. Monitoring of offshore geological carbon storage integrity: implications of natural variability in the marine system and the assessment of anomaly detection criteria. Int. J. Greenh. Gas Control. 64, 99–112.

Blackford, J., Alendal, G., Avlesen, H., Brereton, A., Cazenave, P.W., Chen, B., Dewar, M., Holt, J., Phelps, J., 2020. Impact and detectability of hypothetical CCS offshore seep scenarios as an aid to storage assurance and risk assessment. Int. J. Greenh. Gas Control. 95, 102949.

Caramanna, G., Fietzek, P., Maroto-Valer, M., 2011. Monitoring techniques of a natural analogue for sub-seabed CO2 leakages. Energy Procedia 4, 3262–3268.

Chabora, E.R., Benson, S.M., 2009. Brine displacement and leakage detection using pressure measurements in aquifers overlying CO2 storage reservoirs. Energy Procedia 1, 2405–2412.

CO2CRC, 2013. The Process of Developing a CO2 Test Injection; Experience to Date and Best Practices. IEAGHG.

Consoli, C.P., Wildgust, N., 2017. Current status of global storage resources. Energy Procedia 114, 4623–4628.

Fiedler, B., Fietzek, P., Vieira, N., Silva, P., Bittig, H.C., Körtzinger, A., 2013. In situ CO2 and O2 measurements on a profiling float. J. Atmos. Oceanic Technol. 30, 112–126.

Fietzek, P., Fiedler, B., Steinhoff, T., Körtzinger, A., 2014. In situ quality assessment of a novel underwater pCO2 sensor based on membrane equilibration and NDIR spectrometry. J. Atmos. Oceanic Technol. 31, 181–196.

Gade, H.G., 1968. Horizontal and vertical exchanges and diffusion in the water masses of the oslo fjord. Helgoländer wissenschaftliche Meeresuntersuchungen 17, 462–475.

Institute, G.C., 2015. Global Status of CCS: 2015. Global CCS Institute, Melbourne.

Jenkins, C., Chadwick, A., Hovorka, S.D., 2015. The state of the art in monitoring and verification—ten years on. Int. J. Greenh. Gas Control. 40, 312–349.

Kampman, N., Bickle, M.J., Maskell, A., Chapman, H.J., Evans, J.P., Purser, G., Zhou, Z., Schaller, M.F., Gattacceca, J.C., Bertier, P., Chen, F., Turchyn, A.V., Assayag, N., Rochelle, C., Ballentine, C.J., Busch, A., 2014. Drilling and sampling a natural CO2 reservoir: implications for fluid flow and CO2-fluid–rock reactions during CO2 migration through the overburden. Chem. Geol. 369, 51–82.

Maeda, Y., Shitashima, K., Sakamoto, A., 2015. Mapping observations using AUV and numerical simulations of leaked CO2 diffusion in sub-seabed CO2 release experiment at Ardmucknish Bay. Int. J. Greenh. Gas Control. 38, 143–152.

Millero, F.J., Chen, C.-T., Bradshaw, A., Schleicher, K., 1980. A new high pressure equation of state for seawater. Deep. Sea Res. Part A Oceanogr. Res. Pap. 27, 255–264.

Miloshevich, L.M., Paukkunen, A., Vömel, H., Oltmans, S.J., 2004. Development and validation of a time-lag correction for vaisala radiosonde humidity measurements. J. Atmos. Oceanic Technol. 21, 1305–1327.

Myers, M.B., Roberts, J.J., White, C., Stalker, L., 2019. An experimental investigation into quantifying CO2 leakage in aqueous environments using chemical tracers. Chem. Geol. 511, 91–99.

Ohsumi, T., Nakashiki, N., Shitashima, K., Hirama, K., 1992. Density change of water due to dissolution of carbon dioxide and near-field behavior of CO2 from a source on deep-sea floor. Energy Convers. Manage. 33, 685–690.

Ohtaki, E., Yamashita, E., Fujiwara, F., 1993. Carbon dioxide in surface seawaters of the Seto Inland Sea, Japan. J. Oceanogr. 49, 295–303.

Phelps, J.J.C., Blackford, J.C., Holt, J.T., Polton, J.A., 2015. Modelling large-scale CO2 leakages in the North Sea. Int. J. Greenh. Gas Control. 38, 210–220.

Pruess, K., 2011. Integrated modeling of CO2 storage and leakage scenarios including transitions between super- and subcritical conditions, and phase change between liquid and gaseous CO2. Greenh. Gases Sci. Technol. 1, 237–247.

Røed, L., 2016. Vertical mixing and internal wave energy fluxes in a sill fjord. J. Mar. Syst. 159.

Schacht, U., Jenkins, C., 2014. Soil gas monitoring of the Otway Project demonstration site in SE Victoria, Australia. Int. J. Greenh. Gas Control. 24, 14–29.

Shitashima, K., Maeda, Y., Sakamoto, A., 2015. Detection and monitoring of leaked CO2 through sediment, water column and atmosphere in a sub-seabed CCS experiment. Int. J. Greenh. Gas Control. 38, 135–142.

Uchimoto, K., Kita, J., Xue, Z., 2017. A novel method to detect CO2 leak in offshore storage: focusing on relationship between dissolved oxygen and partial pressure of CO2 in the sea. Energy Procedia 114, 3771–3777.

Uchimoto, K., Nishimura, M., Kita, J., Xue, Z., 2018. Detecting CO2 leakage at offshore storage sites using the covariance between the partial pressure of CO2 and the saturation of dissolved oxygen in seawater. Int. J. Greenh. Gas Control. 72, 130–137.